

Bernstein-Greene-Kruskal theory of electron holes in superthermal space plasma

Harikrishnan Aravindakshan,^{a)} Amar Kakad,^{b)} and Bharati Kakad^{c)}
Indian Institute of Geomagnetism, New Panvel, Navi Mumbai 410218, India

(Received 8 February 2018; accepted 16 April 2018; published online 9 May 2018)

Several spacecraft missions have observed electron holes (EHs) in Earth's and other planetary magnetospheres. These EHs are modeled with the stationary solutions of Vlasov-Poisson equations, obtained by adopting the Bernstein-Greene-Kruskal (BGK) approach. Through the literature survey, we find that the BGK EHs are modelled by using either thermal distribution function or any statistical distribution derived from particular spacecraft observations. However, Maxwell distributions are quite rare in space plasmas; instead, most of these plasmas are superthermal in nature and generally described by kappa distribution. We have developed a one-dimensional BGK model of EHs for space plasma that follows superthermal kappa distribution. The analytical solution of trapped electron distribution function for such plasmas is derived. The trapped particle distribution function in plasma following kappa distribution is found to be steeper and denser as compared to that for Maxwellian distribution. The width-amplitude relation of perturbation for superthermal plasma is derived and allowed regions of stable BGK solutions are obtained. We find that the stable BGK solutions are better supported by superthermal plasmas compared to that of thermal plasmas for small amplitude perturbations. *Published by AIP Publishing.* <https://doi.org/10.1063/1.5025234>

I. INTRODUCTION

Over the past decade, various space-borne experiments show that the electrostatic solitary waves (ESWs) are ubiquitous in Earth's magnetosphere.^{1–10} These solitary waves are observed as “holes” in phase space. Depending on the trapped species, these holes can be either electron holes (EHs) or ion holes (IHs). The nonlinear treatment of the problem of electrostatic modes in a Vlasov gas was developed by Bernstein, Greene, and Kruskal (BGK).¹¹ Until then this problem was mostly resorted to the linearization of governing equations, leading to a mathematically tractable problem. However, the linear theory breaks down for the particles trapped in the potential energy troughs, as the particle velocity and wave velocity will be comparable. Thus, a nonlinear theory was imperative. In 1956, Bernstein, Greene, and Kruskal solved the time independent Vlasov-Poisson equations and obtained general solutions for nonlinear plasma waves in the electrostatic regime.¹¹ They showed that it is possible to construct nonlinear disturbances of arbitrary shapes by cleverly choosing the distribution of trapped particles. Later in 1967, Roberts and Berk¹² provided a physical picture for phase space EHs in a numerical experiment on nonlinear evolution of two-stream instability. In their model, they considered that the trapped particles follow the Dirac delta distribution. Further, it took more than a decade to experimentally verify the existence of BGK EHs. In 1979, at Risø laboratory, the existence of BGK EHs was confirmed.¹³ Turikov¹⁴ followed the BGK approach and constructed the trapped electron distribution for a Maxwellian ambient electron distribution and various solitary potential

profiles. Later, based on the BGK approach, many theories explaining the fundamental concepts concerning the plasma phenomenon of the electron hole and their application to ESWs observed in space plasmas have been proposed.^{15,16}

Most of the BGK based models assume the space plasma in thermal (Maxwellian) equilibrium, described by the Maxwell distribution. However, this assumption is not valid everywhere in space plasma environments. Space plasmas are rich in various plasma processes like particle acceleration, plasma heating, etc. All these plasmas lead the plasma to deviate from the state of thermal equilibrium.¹⁷ Superthermal particle distributions are ubiquitous in the Earth's magnetosphere, especially regions like radiation belts and auroral region, etc. Also, their presence is confirmed by many spacecraft measurements.¹⁸ These types of distributions are well described by the so-called kappa (κ) or generalized Lorentzian velocity distribution functions, as shown for the first time by Vasyliunas.¹⁹ Such distributions have high-energy tails deviated from a Maxwellian and decreasing as a power law in particle speed. The one-dimensional isotropic kappa velocity distribution function for electron has the following form:²⁰

$$f_e(V) = \frac{n_{0e}}{(\pi\kappa\theta_e^2)^{1/2} \Gamma(\kappa - 1/2)} \left[1 + \frac{V^2}{\kappa\theta_e^2} \right]^{-\kappa}. \quad (1)$$

In the equation above, Γ is the gamma function, and n_{0e} and V are the density and velocity of electrons. $\theta_e^2 = [(\kappa - 3/2)/\kappa]v_{th,e}^2$ is the most probable speed or characteristic speed, where $v_{th,e} = (2k_B T_e/m_e)^{1/2}$ is the thermal speed of the plasma species, and k_B is the Boltzmann constant. T_e and m_e are temperature and mass of the electrons, respectively. The spectral index κ decides the slope of the tail of the distribution function, and it is always greater than 1.5. The smaller

^{a)}harikrishnan15@iigs.iigm.res.in

^{b)}amar@iigs.iigm.res.in

^{c)}ebharati@iigs.iigm.res.in

value of κ enhances the superthermal population in the system, which leads to decrease in the slope of the tail. As the kappa index $\kappa \rightarrow \infty$, the kappa distribution function converges to the Maxwellian distribution function. For the space plasmas,¹⁸ the kappa index is observed in the range $2 < \kappa < 6$. The presence of superthermal particles in space plasmas suggests a possible role in the existence domain and the characteristics of ESWs, which is confirmed by different fluid models.^{21–24} In this paper, we develop a one-dimensional BGK model of EHs in superthermal space plasmas to address the effect of superthermal plasma population on the characteristics of EHs. Further, this paper is organized as follows: In Sec. II, we discuss the mathematical formulation of BGK EH with the superthermal distribution. The width-amplitude relation is detailed in Sec. III, and the present study is summarized and concluded in Sec. IV.

II. MODEL

We consider a one-dimensional collisionless two-component unmagnetized plasma consisting of electrons and ions. The fundamental equations that govern the electrostatic electron holes in such a plasma are Vlasov and Poisson equations

$$\frac{\partial f_s}{\partial t} + V_s \frac{\partial f_s}{\partial x} - \frac{q_s}{m_s} \frac{\partial \Phi}{\partial x} \frac{\partial f_s}{\partial v} = 0, \quad (2)$$

$$\frac{d^2 \Phi}{dx^2} = \frac{-(q_e n_e + q_i n_i)}{\epsilon_0}, \quad (3)$$

where f_s , q_s , V_s , and m_s are the distribution function, charge, velocity, and mass of the species s , respectively. Here $q_e = -e$ for electrons and $q_i = +e$ for ions. n_e and n_i are electron and ion densities. Φ is the electrostatic potential and ϵ_0 is the permittivity of the medium. For simplicity, the ion density is assumed to be uniform. This assumption is justified by the fact that the large mass ratio between ion and electron prevents ions from contributing significantly to electron dynamics. Furthermore, it is convenient to work in a coordinate system in which the electron hole is at rest, the so-called wave frame, so that all quantities are time-independent. In such a case, the equations above then take the following dimensionless form:¹¹

$$v \frac{\partial f_e(v, x)}{\partial x} + \frac{1}{2} \frac{\partial \phi}{\partial x} \frac{\partial f_e(v, x)}{\partial v} = 0, \quad (4)$$

$$\frac{d^2 \phi}{dx^2} = \int_{-\infty}^{\infty} f_e(v, x) dv - 1. \quad (5)$$

In Eq. (5), we have used $n_e = \int_{-\infty}^{\infty} f_e(x, v) dv$, for total number of electrons. Also in the above equations, v is the normalized electron velocity in the frame co-moving with the wave perturbation, and f_e is the electron distribution function. The normalizations used here are such that the energies are normalized by ambient electron thermal energy, $2k_B T_e$. x is normalized by the electron Debye length, $\lambda_{de} = \sqrt{k_B T_e / \epsilon_0 n_0 e^2}$. Velocity is normalized with the electron thermal velocity $v_{th,e} = \sqrt{2k_B T_e / m_e}$, and ϕ is the potential normalized by $k_B T_e / e$. Here, T_e is the electron temperature, k_B is the Boltzmann constant, and n_0 is the equilibrium density of

electrons. We consider superthermal electrons in the model that follow the kappa distribution as given by Eq. (1). The normalized form of Eq. (1) is given by

$$f_e(v) = \frac{\Gamma(\kappa)}{\sqrt{\pi} \Gamma(\kappa - 1/2) \sqrt{\kappa - 3/2}} \left(1 + \frac{v^2}{\kappa - 3/2} \right)^{-\kappa}. \quad (6)$$

Following the BGK scheme, we assume a frame in which both potential pulse and the electron distribution are in a self-consistent steady state. Working in this frame, we write the electron distribution function in terms of the normalized total energy of the particles given by

$$w = \frac{1}{2} (v^2 - \phi). \quad (7)$$

Now, we will make a change of variable $[(x, v) \rightarrow w]$; that is, we will move to the energy frame, w . Thus, the normalized distribution function transforms as

$$f_e(w) = \frac{\Gamma(\kappa)}{\sqrt{\pi} \sqrt{\kappa - 3/2} \Gamma(\kappa - 1/2)} \left(1 + \frac{2w + \phi}{\kappa - 3/2} \right)^{-\kappa}, \quad (8)$$

where

$$f(x, v) dv = f(w) dw / \sqrt{2w + \phi}.$$

Here, the total energy (w) is normalized with $mv_{th,e}^2$, i.e., $2k_B T_e$. As these electrons encounter a positive potential pulse, depending on their respective velocities, some of them will get trapped and some of them will pass through. Hence, two kinds of the population exist. One is the passing electron population (with $w > 0$), and another one is the trapped electron population (with $w < 0$). Passing electrons follow their initial distribution, which in our case is the kappa distribution. The trapped electrons, which oscillate inside the potential, follow a different distribution, which needs to be derived using BGK approach. One key step in the BGK approach is to separate particles that are trapped in the potential, and those that are passing. We assume the form of the potential applied and the form of distribution function for passing particles. Then we solve for the trapped particle distribution function and derive the physical parameter range for stable solutions of EHs. Spacecraft observations show that the wave potential structures of the Gaussian form are a most common in the Earth's magnetosphere.^{1,29} The positive wave potential acts as a perturbation to trap electrons within it. We assume this potential in the Gaussian form given by

$$\phi(x) = \psi \exp\left(-\frac{x^2}{2\delta^2}\right), \quad (9)$$

where ψ is the amplitude, and δ is the width of the perturbation, respectively. δ is a distance, where the potential decreases to 0.6065 times the maximum amplitude of ψ . The full width half maximum of (FWHM) of perturbation is given by, $\Delta = 2.35\delta$. As there are two kinds of electron population (i.e., trapped and passing) exists here, they will have two different distribution functions. The passing particle distribution function is denoted by f_p , and the trapped electron

is denoted by f_{tr} . The net charge density can also be considered as a combination of passing charge density, trapped charged density, and uniform ion background density. Therefore, Eq. (5) can be written as

$$\frac{d^2\phi}{dx^2} = n_p + n_{tr} - 1. \quad (10)$$

In the equation above, n_p is the passing charge density, and n_{tr} is the trapped charged density. The passing electrons are those electrons which are not affected by the potential. For passing electrons, the net energy is always positive, and for the trapped electrons, the energy is assumed to be negative. So those electrons whose velocities fall in the potential range $\pm\sqrt{\phi}$ will get trapped and rest will pass through. This sets the range of integration for both passing and trapped electron distributions. Thus, in terms of distribution function, Eq. (10) can be written as

$$\begin{aligned} \frac{d^2\phi}{dx^2} = & \int_{-\infty}^{-\sqrt{\phi}} f_p(x, v) dv + \int_{+\sqrt{\phi}}^{\infty} f_p(x, v) dv \\ & + \int_{-\sqrt{\phi}}^{+\sqrt{\phi}} f_{tr}(x, v) dv - 1. \end{aligned} \quad (11)$$

In the equation above, we have used

$$n_p = \int_{-\infty}^{-\sqrt{\phi}} f_p(x, v) dv + \int_{+\sqrt{\phi}}^{\infty} f_p(x, v) dv, \quad (12)$$

$$n_{tr} = \int_{-\sqrt{\phi}}^{+\sqrt{\phi}} f_{tr}(x, v) dv. \quad (13)$$

We now rearrange Eq. (11) to obtain the expression for the trapped electron distribution function

$$n_{tr} = \frac{d^2\phi}{dx^2} - \int_{-\infty}^{-\sqrt{\phi}} f_p(x, v) dv - \int_{+\sqrt{\phi}}^{\infty} f_p(x, v) dv + 1. \quad (14)$$

Now in Eq. (14), the terms in RHS are known and can be solved these terms one by one. Equation (12) gives its expression, wherein and we need to solve the integrals. Exploiting the symmetricity of kappa distribution, we can write n_p as

$$n_p = 2 \int_{+\sqrt{\phi}}^{\infty} f_p dv = 2 \left[\int_0^{\infty} f_p dv - \int_0^{\sqrt{\phi}} f_p dv \right]. \quad (15)$$

Thus making such a transformation, we can solve the integral, and we get an analytical expression for n_p as (see Appendix A for details)

$$n_p = \frac{AB^\kappa}{\sqrt{B}} \left[\frac{B^{1/2-\kappa}}{A} - 2B^{-k} \phi^{1/2} {}_2F_1[\kappa, 1/2, 3/2; -\phi/B] \right], \quad (16)$$

where

$$\begin{aligned} A &= \frac{\Gamma(\kappa)}{\Gamma(k-1/2)\sqrt{\pi}}, \\ B &= \kappa - 3/2, \end{aligned}$$

and ${}_2F_1[a, b, c; z]$ is the Gauss hypergeometric function. Substituting Eqs. (9) and (16) in (14), we get trapped electron density as

$$\begin{aligned} n_{tr} = & \frac{x^2\phi}{\delta^4} - \frac{\phi}{\delta^2} + 1 - \frac{AB^\kappa}{\sqrt{B}} \left[\frac{B^{1/2-\kappa}}{A} \right. \\ & \left. - 2B^{-k} \phi^{1/2} {}_2F_1[\kappa, 1/2, 3/2; -\phi/B] \right]. \end{aligned} \quad (17)$$

But from Eq. (13), we can rewrite Eq. (17) as

$$\begin{aligned} \int_{-\sqrt{\phi}}^{+\sqrt{\phi}} f_{tr}(x, v) dv = & \frac{x^2\phi}{\delta^4} - \frac{\phi}{\delta^2} + 1 - \frac{AB^\kappa}{\sqrt{B}} \left[\frac{B^{1/2-\kappa}}{A} \right. \\ & \left. - 2B^{-k} \phi^{1/2} {}_2F_1[\kappa, 1/2, 3/2; -\phi/B] \right], \end{aligned} \quad (18)$$

which can be written as

$$\begin{aligned} 2 \int_0^{+\sqrt{\phi}} f_{tr}(x, v) dv = & \frac{x^2\phi}{\delta^4} - \frac{\phi}{\delta^2} + 1 - \frac{AB^\kappa}{\sqrt{B}} \left[\frac{B^{1/2-\kappa}}{A} \right. \\ & \left. - 2B^{-k} \phi^{1/2} {}_2F_1[\kappa, 1/2, 3/2; -\phi/B] \right]. \end{aligned} \quad (19)$$

To solve this integral equation, we make a change to variable w using Eq. (7) and then we get

$$\begin{aligned} 2 \int_{-\phi/2}^0 \frac{f_{tr}(w)}{\sqrt{2w+\phi}} dw = & \frac{x^2\phi}{\delta^4} - \frac{\phi}{\delta^2} + 1 - \frac{AB^\kappa}{\sqrt{B}} \left[\frac{B^{1/2-\kappa}}{A} \right. \\ & \left. - 2B^{-k} \phi^{1/2} {}_2F_1[\kappa, 1/2, 3/2; -\phi/B] \right]. \end{aligned}$$

As the RHS of above equation is a function of ϕ , we can assume it to be $g(\phi)$. Then, Eq. (19) can be written as

$$2 \int_{-\phi/2}^0 \frac{f_{tr}(w)}{\sqrt{2w+\phi}} dw = g(\phi). \quad (20)$$

The solution of such an integral equation closely follows the method adopted by Chen and Parks.²⁵ This results in the expression of $f_{tr}(w)$. See Appendix B for the detailed derivation of the f_{tr} .

$$\begin{aligned} f_{tr}(w) = & \frac{2\sqrt{2}\sqrt{-w}}{\pi\delta^2} [1 - 2\ln(-8w/\psi)] \\ & + \frac{A}{\sqrt{B}} {}_2F_1[1/2, \kappa, 1; 2w/B]. \end{aligned} \quad (21)$$

The first term in Eq. (21) arises from the net charge density part, and the second term from the passing particle density. It can be observed from the expression for trapped electron density [Eq. (17)] that the first two terms represent the net charge density and the next term emanates from the passing electron density. Similarly, as the trapped electron distribution function is derived from the trapped electron density, the distribution function will have an explicit dependence on

the net charge density. The effect of superthermal population of plasma on f_{tr} is manifested through the second term of Eq. (21). Thus, the EH characteristics are governed by the second term, which ensues from the assumed distribution of plasma. The first term in Eq. (21) insinuates that the charge density term affects only the trapped particle population. This is evident as the first term vanishes and becomes imaginary for $w > 0$. The first term in Eq. (21) tends to 0 as $w \rightarrow 0$, and due to the effect of second term, the net value of the f_{tr} tends to a positive constant. The second term in Eq. (21) has a finite positive value at $w = 0$, and this term monotonically decreases as w takes negative values. As the trapped population exists only for negative energies, the w is restricted to negative values. We find that first term in Eq. (21) has a maxima at $w = -\frac{\psi}{8} \exp(-5/2)$. The end point behaviour of the two terms implies that $f_{tr}(w = 0) < f_{tr}(w = -\frac{\psi}{8} \exp(-5/2))$. Combining the behavior of two terms in f_{tr} , it can be concluded that $f_{tr}(0 > w > -\frac{\psi}{8} \exp(-5/2)) < f_{tr}(w = -\frac{\psi}{8} \exp(-5/2))$. It implies that the trapped particle distribution function f_{tr} has a single peak in the w space as shown in Fig. 2(a), which corresponds to a double peak in velocity space as shown in Fig. 2(b).

We carried out similar mathematical exercise by treating plasma to be in thermal equilibrium and estimated the trapped particle density and distribution function, i.e., n_{tr} and f_{tr} . These expressions are given in Appendix D. It may be noted that the first term of trapped particle distribution function associated with the superthermal plasmas [Eq. (21)] and the thermal plasma [Eq. (D5)] is identical as they emanate from the charge density part, which is common for both cases. However, the second term for both cases is different, which is attributed to thermal and superthermal effects considered in plasma models.

The three dimensional plot of the trapped particle distribution function is given in Fig. 1. In this figure, $f_{tr}(w)$ is

shown in panel (a), (b) and (c) are plotted using Eq. (21), whereas $f_{tr}(w)$ depicted in panel (d) is plotted using Eq. (D5). From Fig. 1, we observe that as the kappa index takes higher values, the f_{tr} manifests itself as the trapped particle distribution function of the thermal plasma. We see that the trapped particle distribution function is deeper for superthermal plasma as they possess higher trapped density. For the thermal plasma, the edges are comparatively less darker, which indicates that the trapped population in thermal plasma is less. This is quite obvious as superthermal plasma that follows kappa distribution has a low average thermal velocity as compared to thermal plasma. The higher depth of superthermal plasma hints us that the electron hole formed is deeper. This also means that superthermal plasma traps more particles with lower thermal energy. For a better understanding, we studied the variation of f_{tr} with the energy variable w , where $w = \frac{1}{2}(v^2 - \phi)$. This is shown in Fig. 2(a). The f_{tr} is plotted for different values of superthermal index, κ . We observe that for $\kappa = 400$ the trapped particle distribution function approaches to that of Maxwellian. In Fig. 2(a), all the four curves tend to converge at one point when $f_{tr}(w)$ approaches zero. This value is $w = -0.35$. This value implies $w = -\psi/2$ and is the center of electron phase space hole where $x = v = 0$. For f_{tr} , $w = -\psi/2$ is a point of global minimum, beyond which f_{tr} becomes negative, which is physically irrelevant for stable BGK EHs. The global minimum implies that the phase space holes have a minimum phase space density at the centers. This can be better understood from Fig. 2(b). Figure 2(b) depicts the variation of f_{tr} in velocity space. It can be observed that there are two peaks in the plot one in the negative axis and other one in the positive axis. This phenomenon manifests itself as two counter-streaming beams with equal magnitude of velocity. With the solitary wave potential, the counter-streaming beams are self-consistent configurations, which have been

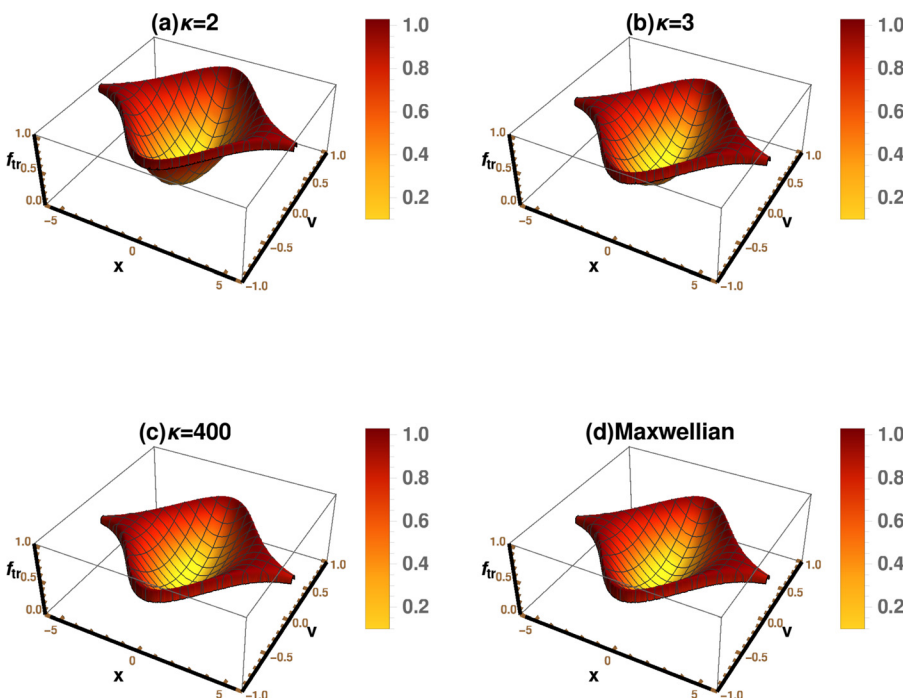


FIG. 1. Plot of trapped electron distribution function f_{tr} in x - v domain. The four panels depict the variation of f_{tr} for various superthermal indexes κ . The colour gradient shows the variation of trapped electron density. Here we have used $\psi = 0.7$ and $\delta = 1.7$.

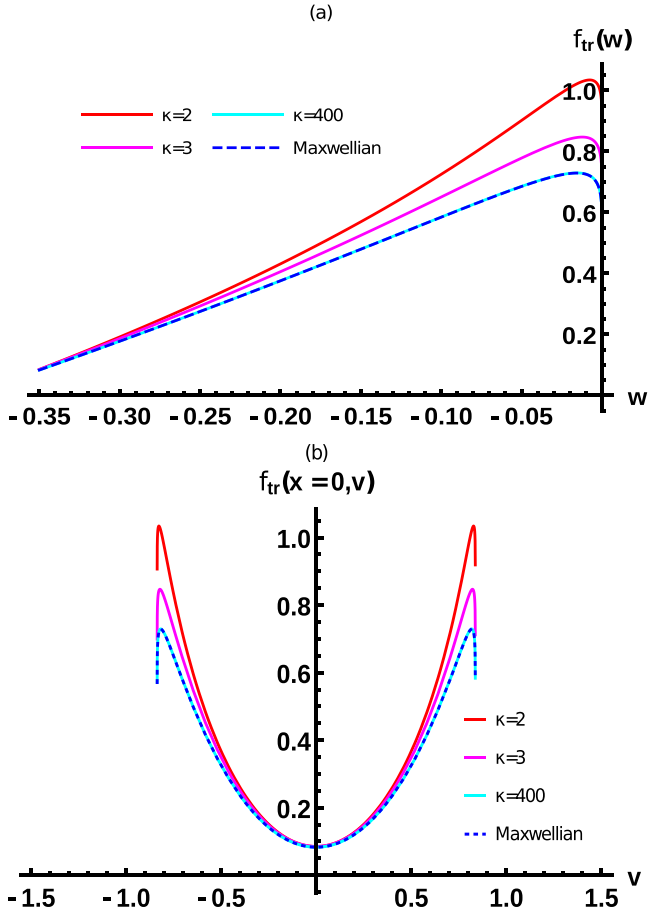


FIG. 2. (a) shows the variation of trapped particle distribution function f_{tr} with the energy variable w for superthermal plasma with $\kappa = 2, 3, 400$, and thermal plasma. The dashed line depicts the case of thermal plasma. (b) shows the corresponding variation of trapped particle distribution function f_{tr} of superthermal plasma for $\kappa = 2, 3, 400$, and thermal plasma in velocity space. Here, $\delta = 1.7$ and $\psi = 0.7$.

demonstrated to be stable by numerical simulations as well as by analytical means.¹⁵

III. WIDTH-AMPLITUDE RELATION FOR SUPERHERMAL PLASMAS

For a stable BGK solution, the trapped electron distribution function should be positive.¹¹ Exploiting this condition, we can derive the allowed regions of width-amplitude relation for the wave potential incorporated in the plasma. In the case of trapped particles, the dominant force they experience will be provided by the potential; hence we can neglect the effects of velocity. Assuming the maximum potential applied, we get $w = -\psi/2$. Using this relation, $f_{tr}(\psi, \delta, w = -\psi/2) \geq 0$ suffices this requirement, yielding the width-amplitude relation for superthermal plasma (see Appendix C for detailed derivation)

$$\delta^2 \geq \frac{2\sqrt{B}}{\pi A} \frac{\sqrt{\psi}(2\ln 4 - 1)}{2F_1[1/2, \kappa, 1, -\psi/B]}. \quad (22)$$

This inequality is represented in Fig. 3(a) for superthermal plasmas [Eq. (22)] and thermal plasmas [Eq. (D6)]. The colored region separates the whole space into stable and

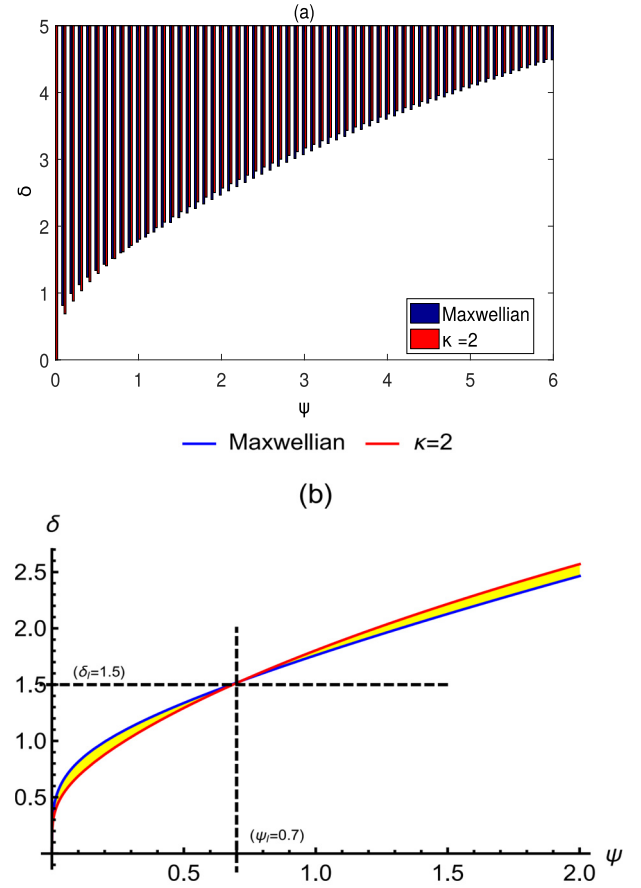


FIG. 3. (a) Allowed regions of width-amplitude for the existence of stable BGK solutions linked with EHS for superthermal (red) and thermal (blue) are shown by vertical bars. (b) The limiting boundary (lowest limit, where stable solution exists) of δ as a function of amplitude of perturbation is shown for superthermal (red) and thermal plasmas (blue). The region shaded with yellow color indicates the deviation of this lower boundary for thermal and superthermal plasmas. The limiting value of δ_l and ψ_l represents the value where thermal and superthermal plasmas have the same allowed regions for amplitude-width of perturbation.

unstable regions. In Fig. 3(a), blue and red color bars, respectively, represent the stability regions for thermal and superthermal plasmas. It is evident from Eq. (22) that the minimum allowed width for stable EHS increases with the potential amplitude, ψ . We observe from Fig. 3(b) that the parametric regime of ψ and δ that supports stable BGK EH solutions in superthermal plasma is greater than that of thermal plasma for perturbation with amplitude $\psi \leq \psi_l$ and width $\delta \leq \delta_l$. But after these ψ and δ of the perturbation, the thermal plasma shows a higher region of stability in comparison with superthermal plasma. We can define these limiting values as $\psi_l - \delta_l$. At this point, the stability regions of both Maxwellian and kappa equalize. It suggests that the perturbation of width $\Delta_l \leq 2.35\delta_l$, i.e., $\Delta_l \leq 3.53\lambda_D$, and amplitude $\psi \leq 0.7e/k_B T$ has a higher region of stability for superthermal plasmas. In order to quantify the difference in the regions, we take the ratio between the width of thermal and superthermal plasmas for $\kappa = 2, 4, 400$. It is depicted from Fig. 4 that for $\psi \leq 0.7$, the stability region for highly superthermal plasma is nearly 25% higher than the thermal plasma. But after $\psi \geq 0.7$, even though the thermal plasma has a higher region of stability, the region

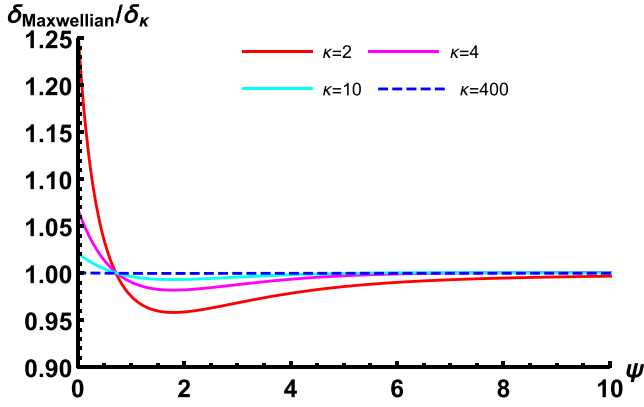


FIG. 4. The ratio of limiting boundary (lowest limit, where stable solution exists) of δ for Maxwellian and superthermal plasma is plotted as a function of amplitude of perturbation. It indicates that the allowed region of stable BGK solutions is nearly 25% more for highly superthermal plasmas ($\kappa=2$) as compared to thermal plasmas.

of thermal plasma is higher by about only 10%. Also at very high amplitude perturbation, none of these differences are significant. We know that the average thermal velocity of particles in superthermal distribution is small compared to thermal plasmas, i.e., $\theta < v_{th}$. The superthermal plasma, which has a large number of lower thermal energy particles than the thermal plasma, will support more BGK solutions for lower perturbations as it has a considerable number of lower energy particles to form stable BGK solutions. But as the perturbation increases, the particles with higher thermal energy will also get trapped. In such a case, the thermal plasma will have an increased population of higher thermal particles. Even though the superthermal plasma has a nonzero tail with high energetic particles, they will not get trapped at all in such perturbations. Thus, the thermal plasma possesses a higher region of stability. But we can see that the stability region is higher by only 10%.

IV. CONCLUSION

This paper is an attempt to introduce a general BGK theory that can be used to model EHs in the space plasma. We have derived analytical results for trapped particle density and distribution function for a one-dimensional unmagnetized plasma following superthermal kappa distribution. Such nonthermal distributions are often found to be present in different regions of the magnetosphere. Thus, this model is more generalized to examine the EHs in space plasmas as compared to the earlier BGK model for thermal space plasmas. Assuming the positive nature of trapped particle distribution function, which is an indispensable condition for stability of BGK EHs, we derived the width-amplitude relation. This relation gives the combination of width and amplitude of perturbation that will result in stable BGK EHs. This study leads to a conclusion that the superthermal plasma is able to form stable BGK solutions for smaller perturbations. This is even observed in the fluid simulation by Lotekar, Kakad, and Kakad,²² where they found that the superthermal plasma supports stable solitary wave structures for a larger set of perturbations than the thermal plasma. We also see from the width-

amplitude plot that for a fixed amplitude of perturbation, the set of δ values supported by superthermal plasma is much greater when the amplitude of wave potential is less than $0.7e/k_B T_e$. This means that under the same initial conditions, more modes of BGK waves are supported by superthermal plasma than thermal plasma. Similar results have been obtained by Lotekar, Kakad, and Kakad²³ in their fluid simulation with cold ions and superthermal electrons. This can be understood in two ways. One is that as the average speed in superthermal plasma is lowered, particles will get trapped even for combinations which are not applicable in the case of thermal plasma. Another way of explaining this phenomenon is in terms of the concept of free energy. As proved by Leubner,²⁶ superthermal plasma will have a lower entropy as compared to that of thermal plasma, which in turn means that it has lower free energy. This will hence lead to the formation of stable BGK solutions rather than leading to the case of instability.

The key findings of the present work are the following:

- (i) The analytical expressions for trapped particle density and distribution function are given for superthermal plasmas,
- (ii) stable BGK solutions are better supported by plasmas following superthermal kappa type distributions for EHs of relatively lower amplitude, i.e., $\phi_{max} < 0.7e/k_B T_e$,
- (iii) the effect of superthermal plasma population is significant for EHs of widths less than $3.53\lambda_D$ and amplitude less than $0.7e/k_B T_e$ (i.e., $\psi_l = 0.7e/k_B T_e$, $\Delta_l = 3.53\lambda_D$). Hence, we conclude that we have come up with a general kinetic model that is well equipped to explain the behavior of BGK electron holes in space plasmas. If a region of space plasma is in thermal equilibrium, the present model can be used by setting up higher κ index.

APPENDIX A: SOLUTION TO THE INTEGRALS

Now, Eq. (15) can be expanded as

$$n_p = \frac{2\Gamma(\kappa)}{\sqrt{\pi}\Gamma(\kappa - 1/2)\sqrt{k - 3/2}} \left[\int_0^\infty \left(1 + \frac{v^2}{\kappa - 3/2}\right)^{-\kappa} dv - \int_0^{\sqrt{\phi}} \left(1 + \frac{v^2}{\kappa - 3/2}\right)^{-\kappa} dv \right]. \quad (A1)$$

Let

$$A = \frac{\Gamma(\kappa)}{\Gamma(\kappa - 1/2)\sqrt{\pi}},$$

$$B = \kappa - 3/2.$$

Also by substituting $v^2 = x$ we get

$$n_p = \frac{AB^k}{\sqrt{B}} \left[\int_0^\infty (B + x)^{-\kappa} x^{-1/2} dx - \int_0^\phi (B + x)^{-\kappa} x^{-1/2} dx \right]. \quad (A2)$$

Now using the following identities from the book of table of integrals by Gradshteyn and Ryzhik,²⁷ we obtain Eq. (16)

$$\begin{aligned} & \int_0^\infty x^{\lambda-1} (1+x)^{-\mu+\nu} (x+\gamma)^{-\nu} dx \\ &= \beta[\mu-\lambda, \lambda]_2 F_1[\nu, \mu-\lambda, \mu, 1-\gamma], \\ & \int_0^u x^{\nu-1} (x+\alpha)^\lambda (u-x)^{\mu-1} dx \\ &= \alpha^\lambda u^{\mu+\nu-1} \beta[\mu, \nu]_2 F_1[-\lambda, \nu, \mu+\nu, -u/\alpha], \end{aligned}$$

where

$$\beta[x, y] = \frac{\Gamma[x]\Gamma[y]}{\Gamma[x+y]}. \quad (\text{A3})$$

We also used the relation for Gauss Hypergeometric function²⁹

$${}_2F_1[\kappa, \kappa-1/2, \kappa, 1-B] = B^{1/2-\kappa}. \quad (\text{A4})$$

APPENDIX B: SOLUTION TO INTEGRAL EQUATION

As mentioned in Eq. (20), we need to solve the following integral equation:

$$2 \int_{-\phi/2}^0 \frac{f_{tr}(w)}{\sqrt{2w+\phi}} dw = g(\phi). \quad (\text{B1})$$

By substituting $2w = -p$, we change the above equation into

$$\int_0^\phi \frac{f_{tr}(-p)}{\sqrt{-p+\phi}} dp = g(\phi). \quad (\text{B2})$$

Now we need to solve for $f_{tr}(-p)$. For that we multiply the above equation by $\frac{1}{\sqrt{\alpha-\phi}}$ and integrate over ϕ from 0 to α . Thus, we get

$$\int_0^\alpha d\phi \frac{g(\phi)}{\sqrt{\alpha-\phi}} = \int_0^\alpha d\phi \int_0^\phi \frac{f_{tr}(-p)}{\sqrt{\alpha-\phi}\sqrt{\phi-p}} dp. \quad (\text{B3})$$

The above equation can be written as

$$\int_0^\alpha d\phi \frac{g(\phi)}{\sqrt{\alpha-\phi}} = \int_0^\alpha dp \int_p^\alpha \frac{f_{tr}(-p)}{\sqrt{\alpha-\phi}\sqrt{\phi-p}} d\phi, \quad (\text{B4})$$

$$\int_0^\alpha d\phi \frac{g(\phi)}{\sqrt{\alpha-\phi}} = \int_0^\alpha f_{tr}(-p) dp \int_p^\alpha \frac{1}{\sqrt{(\alpha-\phi)(\phi-p)}} d\phi. \quad (\text{B5})$$

The second integral in Eq. (B5) becomes π (table of integrals by Gradshteyn and Ryzhik²⁷). Therefore, we have

$$\int_0^\alpha f(-p) dp = \frac{1}{\pi} \int_0^\alpha \frac{g(\phi)}{\sqrt{\alpha-\phi}} d\phi. \quad (\text{B6})$$

Let us consider $p = \alpha$ and the derivative of the above equation with respect to α , we get

$$f(-\alpha) = \frac{1}{\pi} \frac{d}{d\alpha} \left[\int_0^\alpha \frac{g(\phi)}{\sqrt{\alpha-\phi}} d\phi \right]. \quad (\text{B7})$$

Now we use integration by parts and obtain

$$f(-\alpha) = \frac{1}{\pi} \left[\frac{g(0)}{\sqrt{\alpha}} + \int_0^\alpha d\phi \frac{g'(\phi)}{\sqrt{\alpha-\phi}} \right]. \quad (\text{B8})$$

We know that $g(\phi)$ is the trapped electron density and has no value if there is no applied potential. Thus, $g(0) \rightarrow 0$. Also, upon change of variable $\alpha \rightarrow -2w$ we get

$$f_{tr}(w) = \frac{1}{\pi} \int_0^{-2w} \frac{d\phi}{\sqrt{-2w-\phi}} \frac{dg(\phi)}{d\phi}. \quad (\text{B9})$$

We have derived a solution to the integral equation. Now we need to apply this equation to find out the trapped particle distribution function for superthermal plasmas. As a first step, we need to differentiate the trapped particle density given by Eq. (17) with respect to ϕ

$$\begin{aligned} \frac{dg(\phi)}{d\phi} &= \frac{d}{d\phi} \left[\frac{1}{\delta^2} (-2\phi \ln(\phi/\psi) - \phi) + 1 - \frac{AB^\kappa}{\sqrt{B}} \left[\frac{B^{1/2-\kappa}}{A} \right. \right. \\ &\quad \left. \left. - 2B^{-\kappa} \phi^{1/2} {}_2F_1[\kappa, 1/2, 3/2; -\phi/B] \right] \right], \end{aligned} \quad (\text{B10})$$

which is

$$\frac{dg(\phi)}{d\phi} = \frac{-2}{\delta^2} [1 + \ln(\phi/\psi)] - \frac{1}{\delta^2} + \frac{A}{\sqrt{B}} \phi^{-1/2} \left[1 + \frac{\phi}{B} \right]^{-k}. \quad (\text{B11})$$

Substituting Eq. (B11) in Eq. (B9), we get the analytical form of trapped particle distribution function for superthermal plasmas as

$$\begin{aligned} f_{tr}(w) &= \frac{2\sqrt{2}\sqrt{-w}}{\pi\delta^2} [1 - 2\ln(-8w/\psi)] \\ &\quad + \frac{A}{\sqrt{B}} {}_2F_1[1/2, \kappa, 1; 2w/B]. \end{aligned} \quad (\text{B12})$$

To derive Eqs. (B11) and (B12) we have used the following identities:²⁸

1. $\frac{d}{dz} (z^a {}_2F_1[a, b, a+1, -z/n]) = az^{-1+a} \left(1 + \frac{z}{n} \right)^{-b}. \quad (\text{B13})$

2. $\int_0^u x^{\nu-1} (x+\alpha)^\lambda (u-x)^{\mu-1} dx = \alpha^\lambda u^{\mu+\nu-1} \beta[\mu, \nu]_2 F_1[-\lambda, \nu, \mu+\nu, -u/\alpha]. \quad (\text{B14})$

APPENDIX C: DERIVATION OF WIDTH-AMPLITUDE RELATION

Now, we have the trapped particle distribution function given by

$$\begin{aligned} f_{tr}(w) &= \frac{2\sqrt{2}\sqrt{-w}}{\pi\delta^2} [1 - 2\ln(-8w/\psi)] \\ &\quad + AB^{-1/2} {}_2F_1[1/2, \kappa, 1; 2w/B]. \end{aligned} \quad (\text{C1})$$

To obtain the width-amplitude relation, we assume that the trapped particle distribution function is positive, i.e., $f_{tr} \geq 0$. In fact, we are essentially deriving the region of width and amplitude of perturbation that results in a positive distribution function. Also, we have a relation $2w = v^2 - \phi$. In the case of trapped electrons, we assume that the kinetic energy is less than the potential energy. This is a valid assumption because only those particles with lower kinetic energy will get trapped. The moment they get trapped, they will be under the influence of trapping potential, and hence those particles will have more potential energy than the kinetic energy. Hence, we can take $\phi = -2w$. To obtain allowed regions of width-amplitude for stable EHs, we need to take the case $\phi \rightarrow \phi_{max}$, i.e., $\phi = \psi$ which gives us $w = -\psi/2$, i.e., net energy equal to the maximum potential. Applying these assumptions in Eq. (C1), we get

$$\frac{-2\sqrt{\psi}}{\pi\delta^2} [1 - 2\ln 4] \geq -\frac{A}{\sqrt{B} {}_2F_1[k, 1/2, 1, -\psi/B]}. \quad (C2)$$

By rearranging this equation, we get the width-amplitude relation

$$\delta^2 \geq \frac{2\sqrt{B}}{\pi A} \frac{\sqrt{\psi}(2\ln 4 - 1)}{{}_2F_1[1/2, \kappa, 1, -\psi/B]}. \quad (C3)$$

APPENDIX D: DERIVATION OF BGK THEORY FOR THERMAL PLASMA

We here briefly discuss about the derivation of BGK solutions for thermal plasma. Here, we assume the normalized form of the Maxwell-Boltzmann distribution, given by

$$f(v) = \frac{1}{\sqrt{\pi}} \exp(-v^2). \quad (D1)$$

Now, the passing particle density is given by

$$n_p = \int_{-\infty}^{-\sqrt{\phi}} f_p(v) dv + \int_{+\sqrt{\phi}}^{\infty} f_p(v) dv. \quad (D2)$$

Assuming the Maxwell distribution, we get

$$n_p = 1 - \operatorname{erf}[\sqrt{\phi}]. \quad (D3)$$

Substituting this in Eq. (10) and rearranging, we get the trapped particle density for thermal plasma

$$n_{tr} = \frac{x^2\phi}{\delta^4} - \frac{\phi}{\delta^2} + \operatorname{erf}(\sqrt{\phi}). \quad (D4)$$

Now by closely following the same steps, we get the trapped particle distribution function for the thermal plasma

$$f_{tr}(w) = \frac{2\sqrt{2}\sqrt{-w}}{\pi\delta^2} \left[1 - 2\ln\left(-\frac{8w}{\psi}\right) \right] + \frac{\exp(w)I_0(w)}{\sqrt{\pi}}, \quad (D5)$$

where erf is the error function and I_0 is the modified Bessel function of first kind.

Following the same procedure discussed in Appendix C, we derive the width-amplitude relation for thermal plasma

$$\delta^2 \geq \frac{2\sqrt{\psi}(2\ln 4 - 1)}{\sqrt{\pi} \exp\left(-\frac{\psi}{2}\right) I_0\left(-\frac{\psi}{2}\right)}. \quad (D6)$$

- ¹H. Matsumoto, H. Kojima, T. Miyatake, Y. Omura, M. Okada, I. Nagano, and M. Tsutsui, "Electrostatic solitary waves (esw) in the magnetotail: Ben wave forms observed by geotail," *Geophys. Res. Lett.* **21**, 2915–2918, <https://doi.org/10.1029/94GL01284> (1994).
- ²S. Bale, P. Kellogg, D. Larsen, R. Lin, K. Goetz, and R. Lepping, "Bipolar electrostatic structures in the shock transition region: Evidence of electron phase space holes," *Geophys. Res. Lett.* **25**, 2929–2932, <https://doi.org/10.1029/98GL02111> (1998).
- ³R. Ergun, C. Carlson, J. McFadden, F. Mozer, G. Delory, W. Peria, C. Chaston, M. Temerin, R. Elphic, R. Strangeway *et al.*, "Fast satellite observations of electric field structures in the auroral zone," *Geophys. Res. Lett.* **25**, 2025–2028, <https://doi.org/10.1029/98GL00635> (1998).
- ⁴C. Cattell, J. Dombek, J. Wygant, M. Hudson, F. Mozer, M. Temerin, W. Peterson, C. Kletzing, C. Russell, and R. Pfaff, "Comparisons of polar satellite observations of solitary wave velocities in the plasma sheet boundary and the high altitude cusp to those in the auroral zone," *Geophys. Res. Lett.* **26**, 425–428, <https://doi.org/10.1029/1998GL900304> (1999).
- ⁵J. R. Franz, P. M. Kintner, and J. S. Pickett, "Polar observations of coherent electric field structures," *Geophys. Res. Lett.* **25**, 1277–1280, <https://doi.org/10.1029/98GL50870> (1998).
- ⁶H. Matsumoto, X. Deng, H. Kojima, and R. Anderson, "Observation of electrostatic solitary waves associated with reconnection on the dayside magnetopause boundary," *Geophys. Res. Lett.* **30**, 1326, <https://doi.org/10.1029/2002GL016319> (2003).
- ⁷A. Kakad, S. Singh, R. Reddy, G. Lakhina, and S. Tagare, "Electron acoustic solitary waves in the earth's magnetotail region," *Adv. Space Res.* **43**, 1945–1949 (2009).
- ⁸A. Kakad, B. Kakad, C. Anekallu, G. Lakhina, Y. Omura, and A. Fazakerley, "Slow electrostatic solitary waves in earth's plasma sheet boundary layer," *J. Geophys. Res.: Space Phys.* **121**, 4452–4465, <https://doi.org/10.1002/2016JA022365> (2016).
- ⁹G. Lakhina, S. Singh, A. Kakad, and J. Pickett, "Generation of electrostatic solitary waves in the plasma sheet boundary layer," *J. Geophys. Res.: Space Phys.* **116**, A10218, <https://doi.org/10.1029/2011JA016700> (2011).
- ¹⁰G. Lakhina, S. Singh, A. Kakad, M. Goldstein, A. Vinas, and J. Pickett, "A mechanism for electrostatic solitary structures in the earth's magnetosheath," *J. Geophys. Res.: Space Phys.* **114**, A09212, <https://doi.org/10.1029/2009JA014306> (2009).
- ¹¹I. B. Bernstein, J. M. Greene, and M. D. Kruskal, "Exact nonlinear plasma oscillations," *Phys. Rev.* **108**, 546 (1957).
- ¹²K. Roberts and H. Berk, "Nonlinear evolution of a two-stream instability," *Phys. Rev. Lett.* **19**, 297 (1967).
- ¹³K. Saeki, P. Michelsen, H. Pécseli, and J. J. Rasmussen, "Formation and coalescence of electron solitary holes," *Phys. Rev. Lett.* **42**, 501 (1979).
- ¹⁴V. Turikov, "Electron phase space holes as localized bgk solutions," *Phys. Scr.* **30**, 73 (1984).
- ¹⁵L.-J. Chen, "Bernstein-Greene-Kruskal solitary waves in collisionless plasma," Ph.D. dissertation (University of Washington, Seattle, 2002).
- ¹⁶V. Krasovsky, H. Matsumoto, and Y. Omura, "Electrostatic solitary waves as collective charges in a magnetospheric plasma: Physical structure and properties of bernstein-greenekruskal (bgk) solitons," *J. Geophys. Res.: Space Phys.* **108**, 1117, <https://doi.org/10.1029/2001JA000277> (2003).
- ¹⁷G. Livadiotis and D. McComas, "Understanding kappa distributions: A toolbox for space science and astrophysics," *Space Sci. Rev.* **175**, 183–214 (2013).
- ¹⁸V. Pierrard and M. Lazar, "Kappa distributions: Theory and applications in space plasmas," *Sol. Phys.* **267**, 153–174 (2010).
- ¹⁹V. M. Vasyliunas, "A survey of low-energy electrons in the evening sector of the magnetosphere with ogo 1 and ogo 3," *J. Geophys. Res.* **73**, 2839–2884, <https://doi.org/10.1029/JA073i009p02839> (1968).
- ²⁰D. Summers and R. M. Thorne, "The modified plasma dispersion function," *Phys. Fluids B: Plasma Phys.* **3**, 1835–1847 (1991).
- ²¹N. Saini, I. Kourakis, and M. Hellberg, "Arbitrary amplitude ion-acoustic solitary excitations in the presence of excess superthermal electrons," *Phys. Plasmas* **16**, 062903 (2009).

- ²²A. Lotekar, A. Kakad, and B. Kakad, "Fluid simulation of dispersive and nondispersive ion acoustic waves in the presence of superthermal electrons," *Phys. Plasmas* **23**, 102108 (2016).
- ²³A. Lotekar, A. Kakad, and B. Kakad, "Generation of ion acoustic solitary waves through wave breaking in superthermal plasmas," *Phys. Plasmas* **24**, 102127 (2017).
- ²⁴A. Kakad, A. Lotekar, and B. Kakad, "First-ever model simulation of the new subclass of solitons "supersolitons" in plasma," *Phys. Plasmas* **23**, 110702 (2016).
- ²⁵L.-J. Chen and G. Parks, "B_{gk} electron solitary waves: 1d and 3d," *Nonlinear Processes Geophys.* **9**, 111–119 (2002).
- ²⁶M. P. Leubner, "A nonextensive entropy approach to kappa-distributions," *Astrophys. Space Sci.* **282**, 573–579 (2002).
- ²⁷I. S. Gradshteyn and I. M. Ryzhik, *Table of Integrals, Series, and Products* (Academic Press, 2014).
- ²⁸M. Abramowitz and I. A. Stegun, *Handbook of Mathematical Functions: With Formulas, Graphs, and Mathematical Tables* (Courier Corporation, 1964), Vol. 55.
- ²⁹B. Kakad, A. Kakad, and Y. Omura, "Nonlinear evolution of ion acoustic solitary waves in space plasmas: Fluid and particle-in-cell simulations," *J. Geophys. Res.: Space Phys.* **119**, 5589–5599, <https://doi.org/10.1002/2014JA019798> (2014).